TECHNICAL NOTES

NATIONAL ADVISORY COMMITTEE FOR AERONAUTICS.

No. 53.

SIMILITUDE TESTS ON WING SECTIONS.

By

H. Kumbruch.

Translated from the German
By D. L. Bacon,
Langley Memorial Aeronautical Laboratory, N.A.C.A.,
Langley Field, Va.

April, 1921.

NATIONAL ADVISORY COMMITTEE FOR AERONAUTICS.

TECHNICAL NOTE NO. 53.

SIMILITUDE TESTS ON WING SECTIONS.*

By

H. Kumbruch.

Translated from the German
by
D. L. Bacon, L.M.A.L., N.A.C.A.

The application of the results of model tests to full size construction assumes either that the resistance varies as the square of the speed within the range of speeds in question or that the mechanical similarity law is fulfilled by the model test. This latter requires, in addition to geometrical similarity, that the relation of the airflow to the model, both geometrically and mechanically, be exactly like that for the large machine.

This relation holds, as Reynolds has shown, when the expression $\frac{v\,t}{\upsilon}$, the so-called "Reynolds number" is the same both for the model test and for actual flight. Here v signifies air or flying speed, t a linear dimension of the body, in this case the wing chord, υ the kinematic viscosity of the medium in which the motion takes place ($\upsilon = \frac{\text{Viscosity}}{\text{Density}}$). If, as in the usual case, the model is tested in the same medium as that in which the body is later to be propelled; then υ is constant except for comparatively small changes with pressure

* Sonderabdruck aus "Zeitschrift für Flugtechnik und Motorluftschiffahrt" 1919, Heft 9 u. 10.

and temperature, so that the law of similarity is fulfilled when the parameter $E = vt$ is the same in both cases.* For various sized but geometrically similar bodies with the same parameter the same air forces will be developed. Unfortunately it often occurs that the parameter for full flight can not be duplicated in the tunnel, because either the model would have to be too large or the required wind speed is not attainable.** In such cases one must be content to determine the relations between Lift and Drag coefficients and the parameter up to the highest possible values of vt and to extrapolate for the forces on the actual machine.

The law of squared resistances states that air forces are proportional to the square of the velocity. This leads to the following formulas for lift and drag coefficients:***

$$\text{Drag} = c_w F \frac{\gamma}{2g} v^2 = c_w F q$$

$$\text{Lift} = c_a F \frac{\gamma}{2g} v^2 = c_a F q^3$$

---

* The numerical value of the parameter is here taken as the velocity in meters per second multiplied by the specified linear dimensions in millimeters. (The Reynolds number, an absolute coefficient, is about 70 times greater.)

** This method falls down even if very high wind speeds are attainable because of the critical ranges governed by the compressibility of air and hence by the variable V rather than the product Vl (See Prandtl's comment on high speed research by Caldwell and Fales, and blue print A5 from Paris Office, N.A.C.A.) DLB.

*** c_a = lift coefficient
c_w = drag coefficient
F = wing area in m²
γ = specific gravity of air Kg/m³
v = air speed m/sec.
$q = \frac{\gamma}{2g} v^2$
t = chord
b = span
$E(\frac{m}{sec.} .mm) = 93 \times vt \ (\frac{ft^2}{sec})$

in which c_w and c_a are seen to be constant for a constant angle of incidence. Several earlier works on the investigation of the resistance of various bodies* have demonstrated that this law does not hold for all speeds. Sudden discontinuous variations of the values for c_a and c_w at certain "critical" air speeds and also gradual changes of these values if plotted against vt are noticeable. In the first of the reports referred to examples of each kind are given. First, the discontinuous changes were thoroughly investigated and it was found that the more slender the body under test the lower the value of the parameter corresponding to the point of critical flow. Aerofoils are always slender bodies in this sense. Dimensions of model and speeds of tests must be so chosen that at least a portion of the experimental curve lies above the critical range so that no serious irregularities intervene between the conditions of test and those of full flight.

It is always important to carry out the tests, even with wings, to the highest value of vt possible so that the rate of change of lift and drag coefficients may be plotted against vt for the model and from these the actual full size value may be estimated. This purpose is served by the investigations here reported.

Five different wing curves were investigated.

---

*Prandtl "Der Luftwiederstand von Kugeln, Nachrichten der Gesellschaften der Wissenschaften zu Göttingen," Math.-Phys. Klasse, 1914.
C. Wieselsberger, desgl. Zeitschrift f. Motorl und Flugtechnik, 1914.
M. Munk, Luftwiderstandsmessungen an Streken, T.B. Bd. 1, Heft 4, S.85.

K.W.W. 354
H.W.F. 355 & 356
M.V.A. 357 & 358

Three sizes of model for each curve were built, having the following dimensions:

Span	1500 mm.	Chord	600 mm.
"	1000 "	"	200 "
"	720 "	"	120 "

The large surfaces which were built up like actual airplane wings (of ribs and fabric), were tested between flat walls to minimize interference, the others were tested in a free air stream of circular cross-section. Using those models having a chord of 600 mm. and the highest speed (50 m/sec) now available (1919) a parameter of 30,000 m/sec. × mm. can be reached, with corresponding forces which approach those obtained in actual flight. The smallest wings, 700 × 120 mm., correspond in size to those previously used for investigations of aerofoil sections.

These wings were previously tested in the old tunnel under the former standard conditions of v = about 9 m/sec. E = 1080 m/sec. × mm., and also in the new tunnel at lower and higher speeds. (v = 5, 10, 20, 35 m/sec., and E = 600, 1200, 2400, 4200 m/sec. × mm.) It is thus possible to compare the numerous measurements in the old tunnel with those of the new. In addition to the several values of the parameter, the differences in the air circuits, such as open and enclosed streams, and varying degrees of turbulence in the two tunnels have an appreciable effect. The intermediate size of model (1000 × 200 mm.) have been adopted as standard for routine

wing testing in the new tunnel. These models were tested at speeds of 10, 25 and 40 m/sec., corresponding to a parameter of 2000, 5000 and 8000 m/sec. x mm.

Of the six large wings, two were supplied by the Kaiserlichen Werft, Wilhelmshaven, two by the Hannoverschen Waggonfabrik, and two were made at the Research Laboratory. These were built up in the same manner as actual wings. On the front spar, a 3/4 inch gas pipe, were fastened eight ribs, the outer ones spaced at 250 and the inner ones at 160 mm., while between each pair of these were two or three false ribs, all stiffened by diagonals. The rear spar was wooden. The trailing edges of the two wings from the Hannover Waggonfabrik are formed of a small steel wire, those of the remaining wings are of wood formed to the required profile. The wings from the Hannover Waggonfabrik and from the Research Laboratory are covered with fabric while of those from the Kaiserlichen Werft Wilhelmshaven only one was fabric covered; the second, having the same profile, was covered with wooden veneer, the object of this being to provide a means for measuring the effect of sag in the fabric. The models of the two other series were made in the customary manner from plaster over a metal core. The profiles for these wings were obtained from measurements of the first series. For this purpose the profile was measured on a rib and half way between a pair of ribs and the average value taken. The requirements of geometrical similarity between the large and small models are therefore not strictly fulfilled.

The same objection applies of course to the "surface quality" of the fabric and plaster covered wings. In this respect exact similarity is seldom reached.

In testing the two small models no noteworthy departure was made from customary practice. The methods used in the old tunnel have already been described,* those of the new tunnel correspond with them in the most important features. In both cases the customary measurements of drag, lift and moments were made. The method of testing the large wings is shown in Fig. 1. The wing hangs on eight wires, four being attached to the front spar and four to the rear spar. All eight wires are fastened to a beam G supported on a platform scale by means of which the sum of the wire-pulls, i.e., the total lift, is measured. The position of center of pressure of the resultant was not determined. The wires to the rear spar served as a means to adjust the angle of incidence. The drag was measured by means of the projecting ends of the front spar.

The large wings had, as stated, a 1.5 meter span and the air stream had a width of 2.2 meters. The effect of the restricted width of the air stream on the forces (the law of similitude assumes an air stream of the infinite extent) and the small aspect ratio of the wings (2.5) had to be eliminated. For this purpose, in order to obtain as evenly distributed a flow as possible across all sections of the wing, two vertical walls 2.5 m. long by 2 m. high and extending above the air stream were erected adjacent to the ends of the model wing.

* D. L. Prandtl, Die Bedeutung von Modellversuchen für die Luftschiffahrt und Flugtechnik und die Einrichtung für solche Versuche in Göttingen, Zeitschrift d. Vereines deutscher Ingenieure 1909. S. 1711.

The wing must be brought close to these walls without interfering with the force measurements. To this end two plates S, 960 mm. in diameter were fastened to the overhanging ends of the front spars, flat against the ends of the wing, and clearing the side wall and labyrinth plates D by only three millimeters on each side. Although the difference in pressure between the upper and lower sides of the wing tends to cause a leakage around the wing tip this is effectively prevented by the small clearance and the labyrinth cells.

The end loss is thus eliminated and if the air stream were unbounded, both above and below, the measured drag would be only profile resistance. However, the available depth of air stream is only about 1 meter above and below the wing. Because of the lift produced by the wing, this stream will be deflected through a known angle $\beta = \frac{c_a}{2} \cdot \frac{F}{F'}$*. The relations for the wing in the air stream, which approaches in a straight line, and on flowing off, is deflected at the angle β are very nearly the same as though the air stream were of infinite extent and deflected through an angle $\beta/2$. The resultant air force is then turned through $\beta/2$. We thus have, according to the usual

---

* The angle β may be calculated as follows:
Let the speed of the undisturbed air stream be v, the vertical component of the velocity, produced by the wing (Area F m^2) w, the cross sectional area of the air influenced by the wing, i.e., that portion of the air stream between the vertical walls be F'. The vertical reaction of the diverted air is equal to the lift. The mass of air flowing per second
$M = \frac{\gamma}{g} \cdot F' \cdot v$
Thus $M \cdot w = \frac{\gamma}{g} \cdot F' v \cdot w = \text{Lift} = c_a F \frac{\gamma v^2}{2 g}$,
Hence $w = c_a \frac{F}{F'} \frac{v}{2}$
and consequently, $\tan \beta \cong \beta = \frac{w}{v} = \frac{c_a}{2} \cdot \frac{F}{F'}$.

revolution of wind forces, a resistance analogous to edge resistance.

$$W' = A \cdot \sin \frac{\beta}{2} = \sim A \cdot \frac{\beta}{2}$$

or, substituting the above value of β

$$W' = c_a^2 \cdot \frac{F^2}{4\,F'} \cdot q.$$

which gives

$$c_{w'} = c_a^2 \cdot \frac{F}{4\,F'}$$

in place of

$$c_{w'} = \frac{c_a^2}{\pi} \cdot \frac{t}{b}$$

as for edge resistance.

With the present arrangement (b = 1.5 m., diameter of air stream = 2.2 m., consequently $F' = 3.105\ m^2$) the resistance coefficient is the same as for a wing of 1 : 4.4 aspect ratio in the ideal air stream. A correction is also necessary for the small wings tested in the circular air stream (new tunnel) because of the deflection of the current. A more thorough report on this will be presented later.

In order to prevent any possible contact between parts in the labyrinth construction, the front spar was guided by means of two turnbuckles and a spring C (Fig. 1). The discs S were built so stiff that they did not bend appreciably under the difference in pressure. The inner sides of the discs were covered by sheet metal plates B in order to minimize the undesirable effect of frictional resistance. For the same reason the projecting ends of the front spars were shielded from the wind. The plates were cut away sufficiently to allow

the wing to swing through the desired angle of incidence.

The results of the investigation are given in Tables 1 to 5, and are plotted in Figures 3a to 7a. The curves are drawn upon the customary C_a to C_w axes. All values are reduced for the sake of comparison to an aspect ratio of 1:6.* In Figures 3a to 7a the upper left hand diagram shows the coefficients for the 600 mm. chord wing in the new tunnel, the lower right hand diagram those for the new standard size, 1000 × 200 mm. in the new tunnel, the lower left shows the results from the old standard size, 720 × 120 mm., and the upper right the comparative tests with these models in the new tunnel.

In general the curves (Figs. 3a to 7a) indicate that the characteristic properties of a section sooner or later undergo a sudden change and that this change takes place at a comparatively low value of E. Measurements corresponding to values of E below 600 m/sec. are the only ones that cannot be used. In this region the polar curves assume a new position near that for higher parameters. The effect of the critical point has not yet disappeared however. In consecutive tests widely varying measurements are obtained. In these cases only average values are shown on the polar charts. The polar for the veneered surface of section No. 354 show the same essential characteristics as that of the corresponding fabric covered wing. In Fig. 8 polars for these wings are shown for E = 12,000 and 21,000 m/sec. mm. The effect of sag in the fabric is not noticeable. Incidentally, the sag on this wing is rather small. With a more heavily cambered wing the effect might be more not-

iceable. (* See p. 10)

The considerable decrease of the drag coefficient with increased parameter is striking though not unexpected because of similar results with other bodies. In order to show the manner in which this decrease takes place the drag coefficient has been plotted against the parameter in Figures 3b to 7b, for constant values of the lift coefficient C_a = 0, 40, 80, and 120. The ordinates are for the profile resistance C_{wo}, i.e., the total resistance minus the induced resistance, thus that portion of the abscissae of the polar curve lying between the polar and the parabola. These curves show clearly the action of the law of similitude, for geometrically similar models of varying sizes actually have the same resistance coefficient for equal values of the parameter E. The discrepancies at low parameters and for lift coefficients $C_a = 0$ and $C_a = 120$ are easily explained by imperfect geometrical similarity, both in form and in surface finish. These particular conditions however are of but small practical importance.

The curves show that the parameters used in current practice yield somewhat too high values of the resistance coefficient. A general expression for the value of the resistance coefficient in terms of E is not yet available. As soon as more data are collected the relation between these two quantities will be more carefully investigated. It is noteworthy that the profile resistance coefficients measured for high values of E are noticeably smaller than the frictional resistance coefficients now being used. One might try to explain this by assuming that the discs and labyrinths near the ends

* A. Betz. Einfluss der Spannweite und Flächenbelastung auf Luftkräfte von Tragflächen. T.B.I. Heft 4 S 98

of the wings gave rise to an up wind force because of the pressure difference, thus causing too low resistance measurements to be made. This explanation is unsatisfactory however for at the angle of zero lift, where, because of the absence of pressure difference between the upper and lower surfaces there can surely be no such up wind force, the profile resistance remains just as small, at least as long as the air stream along the pressure side is not turbulent. See for example profile 358 which is the only one the results on which are doubtful. It is also possible that in evaluating the customary frictional resistance coefficient an accurate distinction was not successfully made between profile and frictional resistance. In similitude experiments now being prepared this phenomenon will be more fully investigated. Preparations are likewise being made for research on the frictional resistance of smooth surfaces.*

The lift coefficients depend on the value of the parameter to a much less degree than do the resistance coefficients. (See Figs 3b to 7b). For angles of incidence from 0° to 9°, which is the range of practical interest, and for a parameter greater than 4000 m/sec. mm. the lift coefficient may be assumed independent of the parameter. Below this value the behavior of the different profiles varies. For most of them C_a

* These friction tests have been completed and have confirmed the accuracy of the usual friction coefficient. The cause of the abnormally small profile resistance lies in the fact that the induced resistance (see page 7) caused by the deflection of the air stream was calculated somewhat too large as the influence of the small clearance between the wing and the nozzle (about 1.1 m.) had been neglected. The relationship between C_{wo} and E shown in Figs. 3b to 7b still holds except that the absolute value of C_{wo} is somewhat increased.

decreases with increase of the parameter, while for one (#358) it clearly increases. The law of similitude also applies to this variation in C_a excepting for profile #355. The trailing edge of the large model of this profile was very weak and flexible so that there was a possibility both for incorrect measurement of the angle of incidence and for deformation of the profile under wind pressure. The angles of incidence are less accurately held for the large models than for the medium sized ones because the wires supporting the trailing edge are longer and pass over several pulleys and hence stretch more under load, allowing the wing to turn under the force of the wind, so that the angle of incidence during the test is not exactly the same as that to which it was adjusted in still air. With the smallest models it is not always possible to prevent a small change in angle because of the bending of thin trailing edges. While these errors mean little in themselves they nevertheless largely explain the discrepancies between the curves for the different sized models on the C_a - E charts.

The moment coefficients, depending as they do mostly on the lift, are nearly independent of the parameter.

Finally, it will be noticed that there is a variation in the values of the maximum lift coefficient obtained for various values of the parameter. This is shown on the polar curves and more particularly in Figures 3c - 7c. The large models especially show an increasing maximum for high values of the parameter. A comprehensive explanation can not yet be given for this phenomenon, which is in practice of no importance.

TABLE I

K.W.W.	v m/s	E m/s.mm	C_{wo} for C_a = 0	40	80	120	C_a for α = 0	3	6	9	12	$C_{a\ max.}$
Profile No. 354	5	3000	2.3	0.85	2.9	---	12.6	37.1	58.0	70.6	94.8	105
Model No. 1049	10	6000	2.1	0.75	2.2	---	13.3	35.0	58.6	80.2	100.0	110
b = 1500 mm.	20	12000	1.9	0.55	1.4	---	13.0	35.5	59.8	83.2	103.0	113
t = 600 mm.	35	21000	1.7	0.45	1.1	---	12.8	35.5	59.7	84.4	105.1	114
New Wind Tunnel	50	30000	1.5	0.45	1.0	---	13.2	37.5	62.6	87.6	---	---
Model No. 1081	5	600	2.9	1.25	2.6	---	24.8	45.8	63.0	81.9	93.0	99
b = 720 mm	10	1200	3.5	2.05	2.8	---	18.8	39.6	60.6	79.3	92.6	96
t = 120 mm	20	2400	2.3	1.05	2.3	---	15.2	37.5	59.4	79.3	92.9	101
New Wind Tunnel	35	4200	2.1	0.85	2.2	---	14.2	36.9	58.8	77.8	94.1	103
Model No. 1081												
Old Wind Tunnel	9	1080	2.7	1.45	2.3	---	18.8	39.1	64.2	84.5	99.0	105
Model No. 1135												
b = 1000 mm.	10	2000	2.7	1.45	3.2	---	16.0	37.7	58.8	77.8	90.7	95
t = 200 mm.	25	5000	2.3	1.15	2.5	---	15.2	36.3	58.4	78.6	93.2	99
New Wind Tunnel	40	8000	1.9	0.85	2.2	---	15.1	36.1	57.2	78.0	93.0	99

TABLE 2.

H.W.F.	v	E	C_{wo} for C_a =				C_a for α =					$C_{a\ max}$
	m/s	m/s.mm	0	40	80	120	0	3	6	9	12	
Profile No. 355	5	3000	3.6	1.45	2.6	8.4	38.8	60.0	79.0	96.7	109.8	120
Model No. 1050	10	6000	3.4	0.95	1.7	6.4	36.8	60.0	81.3	100.6	116.6	121
b = 1500 mm.	20	12000	3.0	0.75	1.1	4.7	35.8	61.1	84.3	103.5	120.6	123
t = 600 mm.	35	21000	2.7	0.55	0.8	3.9	34.7	60.0	83.9	103.9	119.4	125
New Wind Tunnel	50	30000	2.4	0.35	0.9	---	31.4	53.7	83.0	105.7	---	
Model No. 1082	5	600	3.4	2.75	3.0	---	28.2	54.0	83.1	95.1	104.3	105
b = 720 mm.	10	1200	3.2	1.35	1.5	---	33.6	59.9	81.3	97.7	109.1	110
t = 120 mm.	20	2400	2.9	0.95	1.5	---	34.3	55.0	76.3	92.2	104.8	105
New Wind Tunnel	35	4200	2.9	0.95	1.5	---	32.1	53.1	74.2	91.3	106.4	110
Model No. 1082 Old Wind Tunnel	9	1080	3.3	1.55	1.8	---	34.6	60.2	82.1	99.2	111.9	115
Model No. 1136												
b = 1000 mm.	10	2000	3.3	1.15	1.4	---	34.8	54.8	75.4	90.6	100.7	105
t = 200 mm.	25	5000	3.5	0.95	1.6	---	32.8	54.2	73.1	90.2	102.3	106
New Wind Tunnel	40	8000	3.5	0.95	1.4	---	30.9	53.5	73.7	91.3	104.5	109

TABLE 3.

H.W.F.	v	E	C_{wo} for C_a =				C_a for α =					$C_{a\,max}$
	m/s	m/s.mm	0	40	80	120	0	3	6	9	12	
Profile No. 356	5	3000	5.7	1.75	1.3	4.0	36.3	60.0	83.3	106.3	118.6	122.0
Model No. 1051	10	6000	5.6	1.95	1.5	2.8	36.2	61.3	85.0	105.4	120.6	135.0
b = 1500 mm.	20	12000	5.3	1.65	1.1	1.9	36.4	63.2	86.9	108.8	127.0	143.0
t = 600 mm.	35	21000	5.3	1.65	1.0	1.8	35.8	62.1	87.0	110.0	127.7	141.0
New Wind Tunnel	50	30000	5.5	1.35	0.8	1.4	32.2	59.9	86.8	105.8	---	---
Model No. 1083	5	600	4.1	2.75	2.2	---	27.3	58.6	86.0	101.5	116.1	116.0
b = 720 mm	10	1200	5.3	2.95	2.0	---	41.3	62.6	84.2	101.8	115.0	118.5
t = 120 mm	20	2400	5.1	2.05	1.4	---	39.3	61.7	83.7	103.7	115.3	119.0
New Wind Tunnel	35	4200	5.2	1.95	1.2	---	37.0	59.4	81.7	100.8	113.9	119.0
Model No. 1083												
Old Wind Tunnel	9	1080	6.0	2.75	1.7	3.1	46.4	69.4	92.3	113.4	126.6	130.0
Model No. 1137												
b = 1000 mm.	10	2000	5.0	1.85	1.3	---	44.0	64.8	86.0	104.8	115.4	117.0
t = 200 mm.	25	5000	5.0	1.55	1.3	---	40.9	59.8	84.8	103.9	115.2	119.0
New Wind Tunnel	40	8000	4.9	1.55	1.3	4.2	39.2	62.3	84.3	103.7	116.5	122.0

TABLE 4.

M.V.A.	v m/s	E m/s.mm	Cwo for C_a = 0	40	80	120	C_a for α = 0	3	6	9	12	C_a max.
Profile No. 357	5	3000	3.8	1.55	1.4	5.8	26.7	47.8	74.9	93.2	115.7	122
Model No. 1052	10	6000	3.6	1.35	0.9	3.3	26.8	49.5	78.8	96.2	117.0	126
b = 1500 mm.	20	12000	3.4	1.05	0.7	2.8	27.3	49.7	76.5	98.7	114.9	128
t = 600 mm.	35	21000	3.4	0.95	0.9	1.9	27.2	50.8	78.5	103.1	126.0	142
New Wind Tunnel	50	30000	3.1	0.45	0.4	---	27.4	52.5	81.8	95.9	---	---
Model No. 1084	5	600	3.6	2.35	3.3	---	35.5	57.8	77.6	89.4	104.3	107
b = 720 mm.	10	1200	3.1	2.15	2.2	---	37.0	58.4	83.0	98.2	114.4	115
t = 120 mm.	20	2400	3.6	1.75	1.4	6.2	30.3	52.6	75.7	98.0	112.6	120
New Wind Tunnel	35	4200	3.7	1.75	2.0	5.4	29.5	44.9	67.0	95.6	113.4	120
Model No. 1084 Old Wind Tunnel	9	1080	4.7	2.15	2.0	4.4	33.8	56.4	81.0	103.2	120.0	122
Model No. 1138												
b = 1000 mm.	10	2000	3.8	1.95	1.6	---	30.0	52.5	75.3	92.8	104.5	107
t = 200 mm.	25	5000	3.4	1.35	1.2	---	28.6	51.2	72.0	92.2	105.8	111
New Wind Tunnel	40	8000	3.4	1.25	1.1	---	28.3	50.8	72.4	92.4	107.4	113

TABLE 5

M.V.A.	v	E	c_{wo} for C_a				C_a for α =					C_a max.
	m/s	m/s.mm	0	40	80	120	-3	0	3	6	9	
Profile No. 358	5	3000	4.3	1.05	1.9	3.0	37.8	61.4	82.3	102.9	121.1	142
Model No. 1053	10	6000	3.5	0175	1.2	2.1	37.6	60.7	83.7	105.9	123.6	150
b = 1500 mm.	20	12000	1.4	0.65	0.9	1.4	36.2	60.7	83.4	107.0	127.0	154
t = 600 mm.	35	21000	0.7	0.55	0.8	1.3	34.8	60.2	84.2	106.8	128.2	165
New Wind Tunnel	50	30000	0.4	0.45	0.4	1.1	31.1	57.7	83.2	107.3	128.2	---
Model No. 1085	5	600	4.3	3.25	7.6	---	20.1	47.2	71.7	71.6	77.8	95
b = 720 mm.	10	1200	2.6	2.25	2.1	3.9	29.5	54.0	74.2	98.0	115.3	131
t = 120 mm.	20	2400	2.3	1.55	1.9	2.9	33.5	56.1	78.2	99.8	119.7	128
New Wind Tunnel	35	4200	1.8	1.15	1.7	2.6	33.2	55.2	76.8	98.9	118.3	128
Model No. 1085												
Old Wind Tunnel	9	1080	2.9	2.25	2.3	2.9	34.7	60.0	82.9	105.0	127.0	141
Model No. 1139												
b = 1000 mm.	10	2000	2.9	1.55	1.4	2.4	37.6	58.9	80.8	100.3	117.7	126
t = 200 mm.	25	5000	2.3	1.15	1.4	2.9	36.6	57.7	80.4	100.9	116.8	127
New Wind Tunnel	40	8000	1.5	0.95	1.1	2.1	35.4	56.9	79.6	101.1	117.6	131

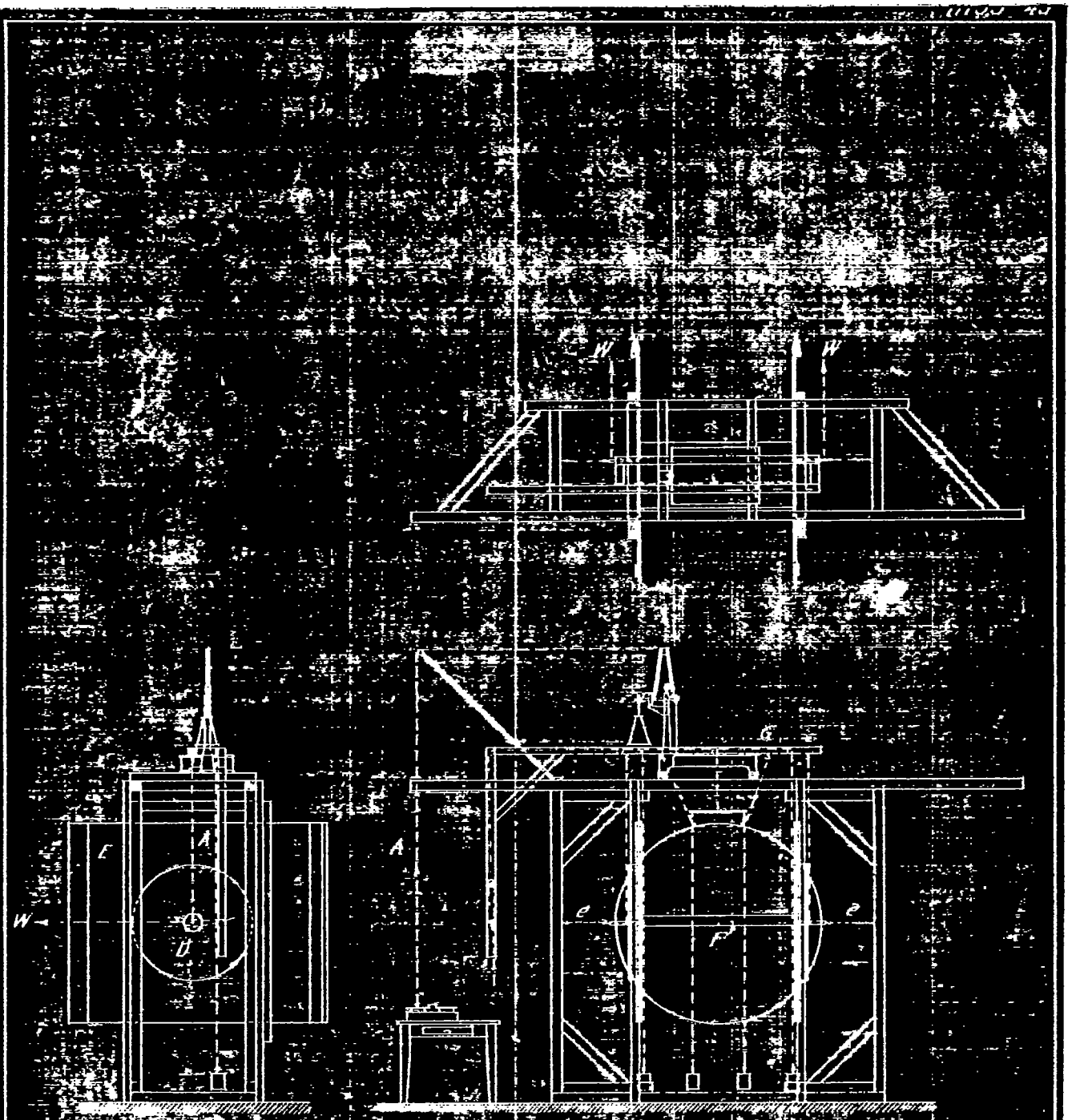

Fig.1 Experimental set-up for tests on large surfaces.

Fig.1

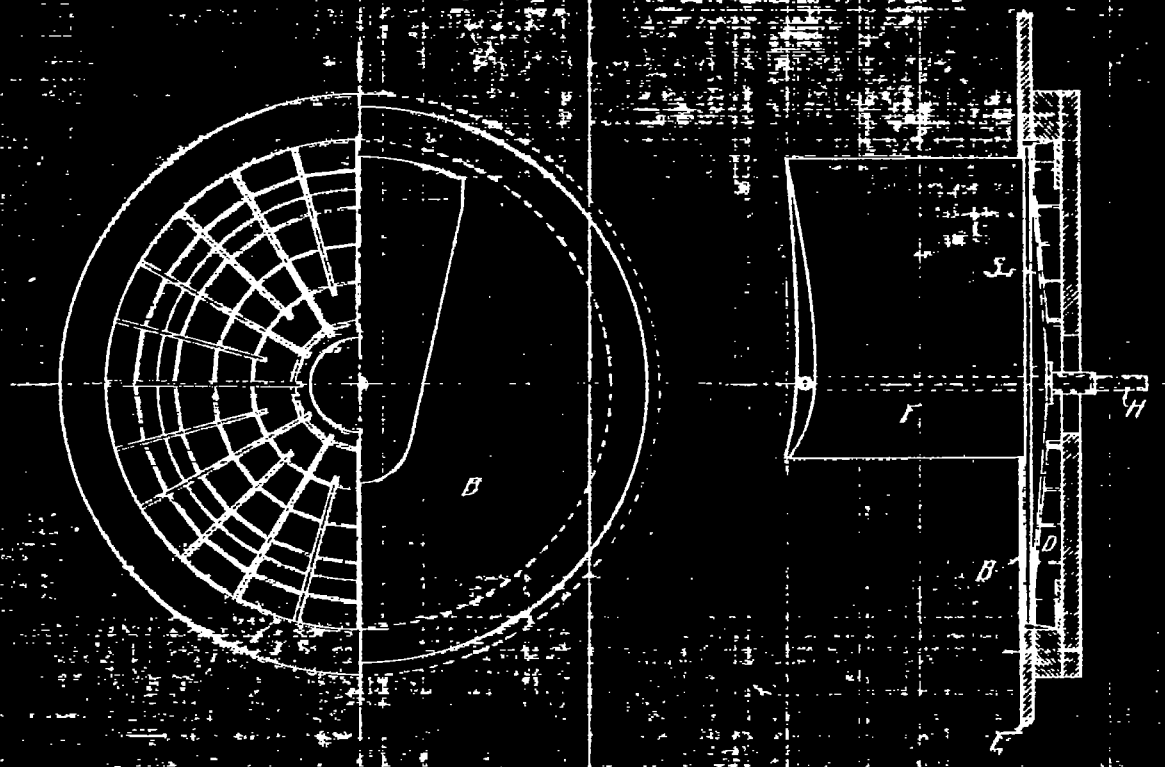

Fig. 2 Side plate attached to tip of model to secure a plane flow. (To eliminate end losses.)

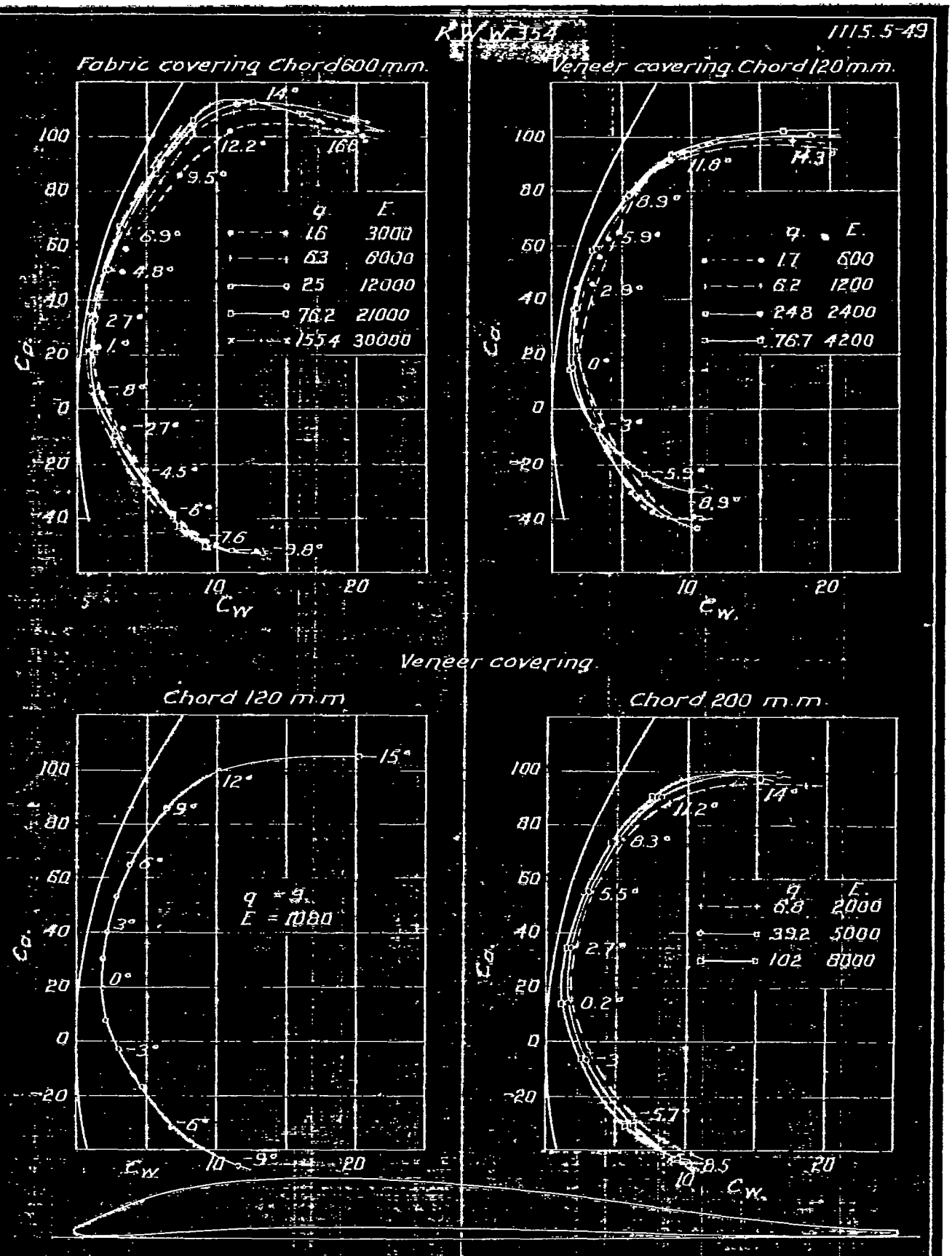
Fabric covering Chord 600 m.m.
Veneer covering. Chord 120 m.m.
Veneer covering.
Chord 120 m.m
Chord 200 m.m.
q E
1.6 3000
6.3 6000
25 12000
76.2 21000
155.4 30000
1.7 600
6.2 1200
24.8 2400
76.7 4200
6.8 2000
39.2 5000
102 8000
q = 9
E = 1080
Cw
Co

Fig. 3a

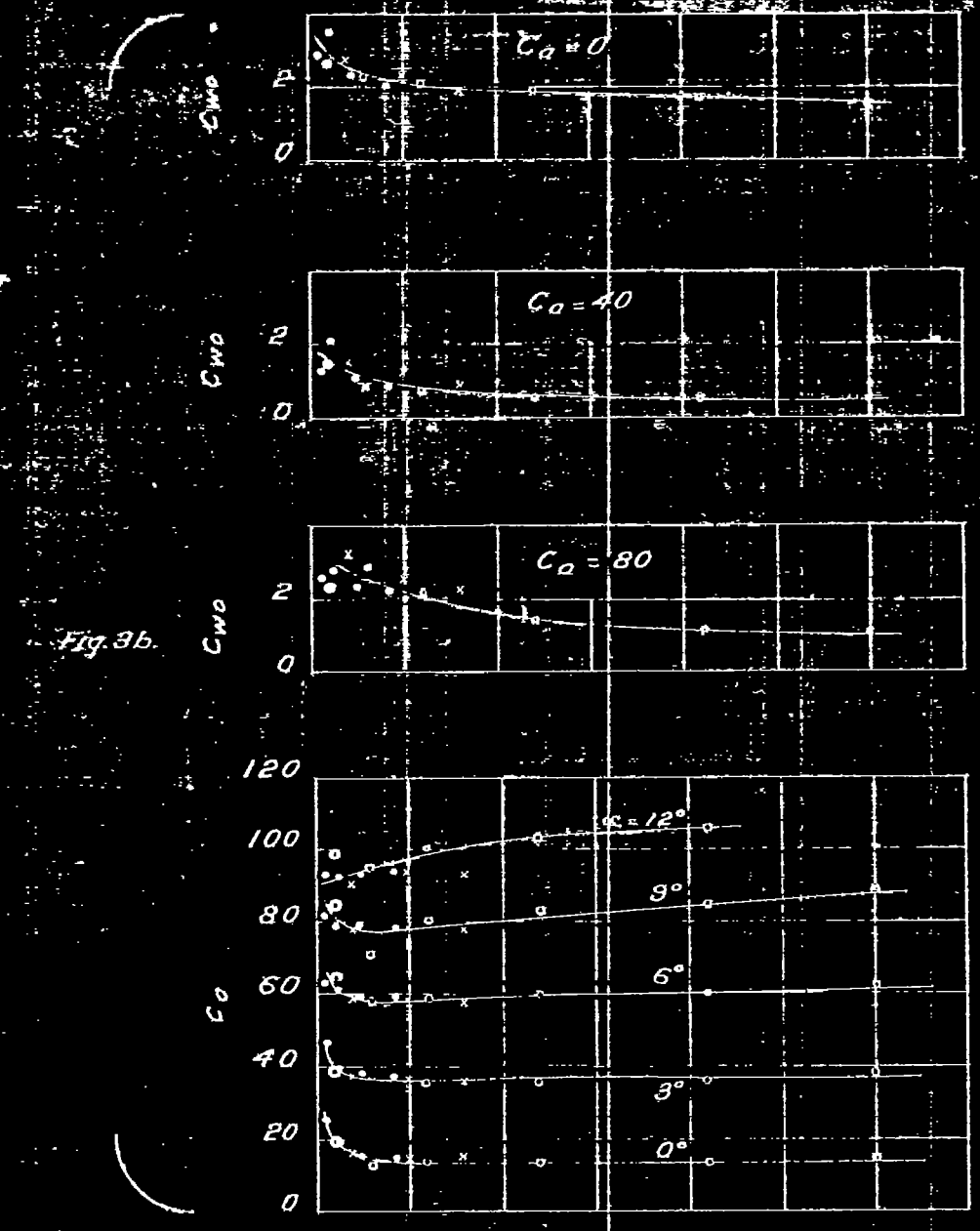
$C_a = 0$
$C_a = 40$
$C_a = 80$
C_{wo}
2
0
Fig. 3b.
120
100
80
60
40
20
0
C_a
$\alpha = 12°$
9°
6°
3°
0°
Fig. 3c.
150
125
100
75
C_a max.
1000
2000
3000
$E = \frac{m}{5 sec.}$ mm.
○ t = 120 mm. Old installation.
• t = 120 mm.
× t = 200 mm.
t = 600 mm.
New installation.

Fig. 3b, 3c.

H.W.E. 355

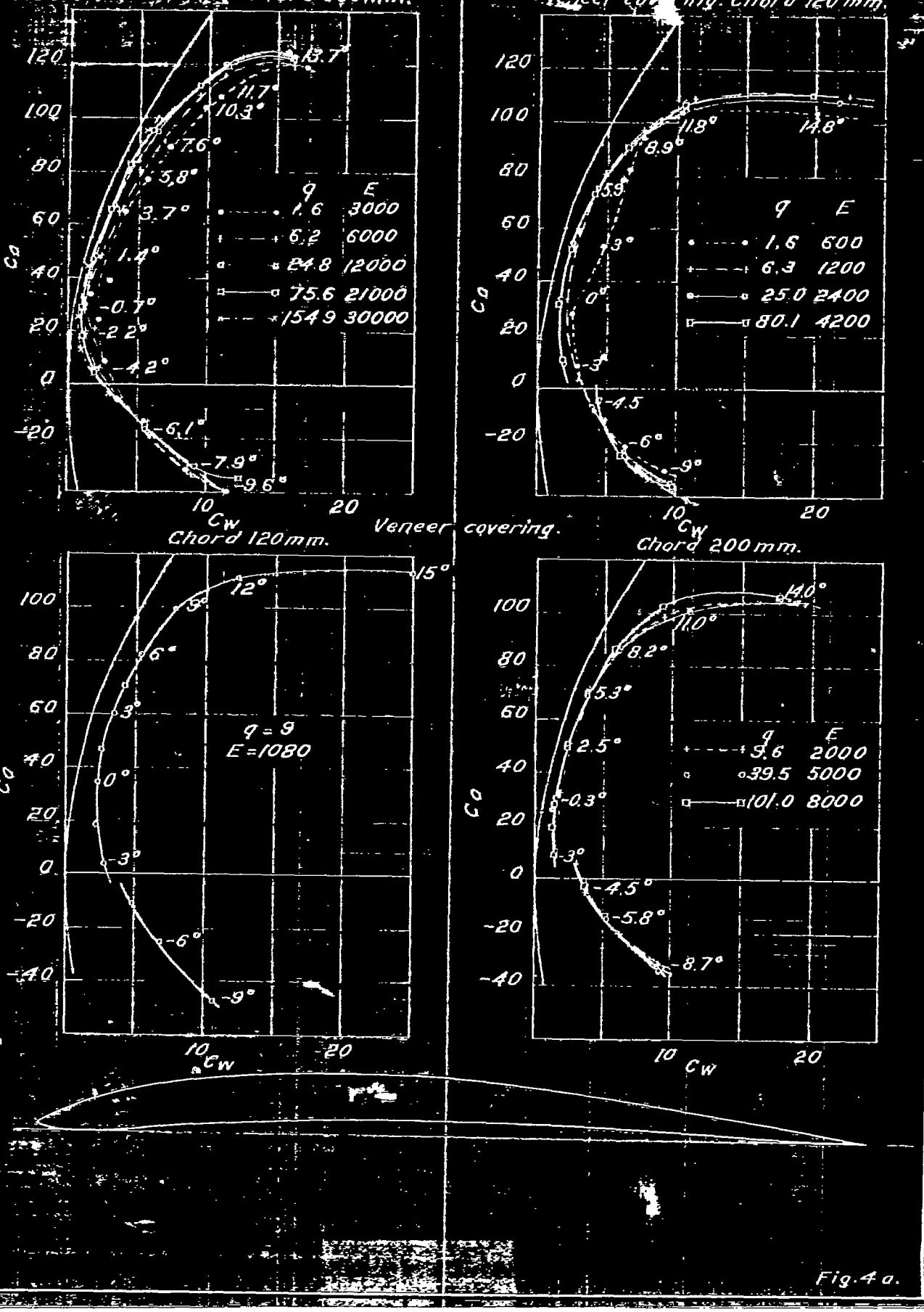

Fig. 4a.

H.W.F. 355.

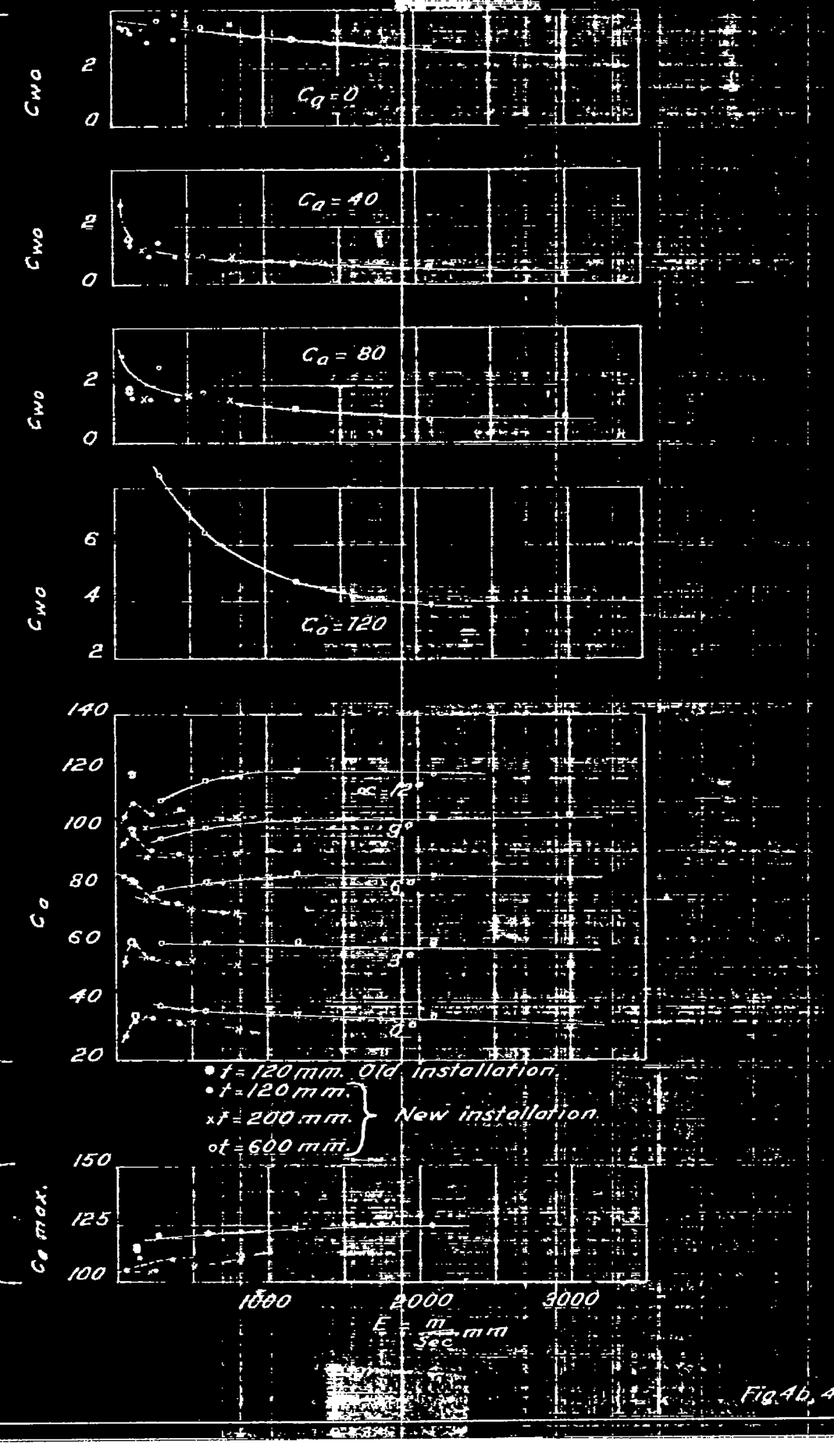

Fig. 4b.

Fig. 4c.

Fig. 4b, 4c.

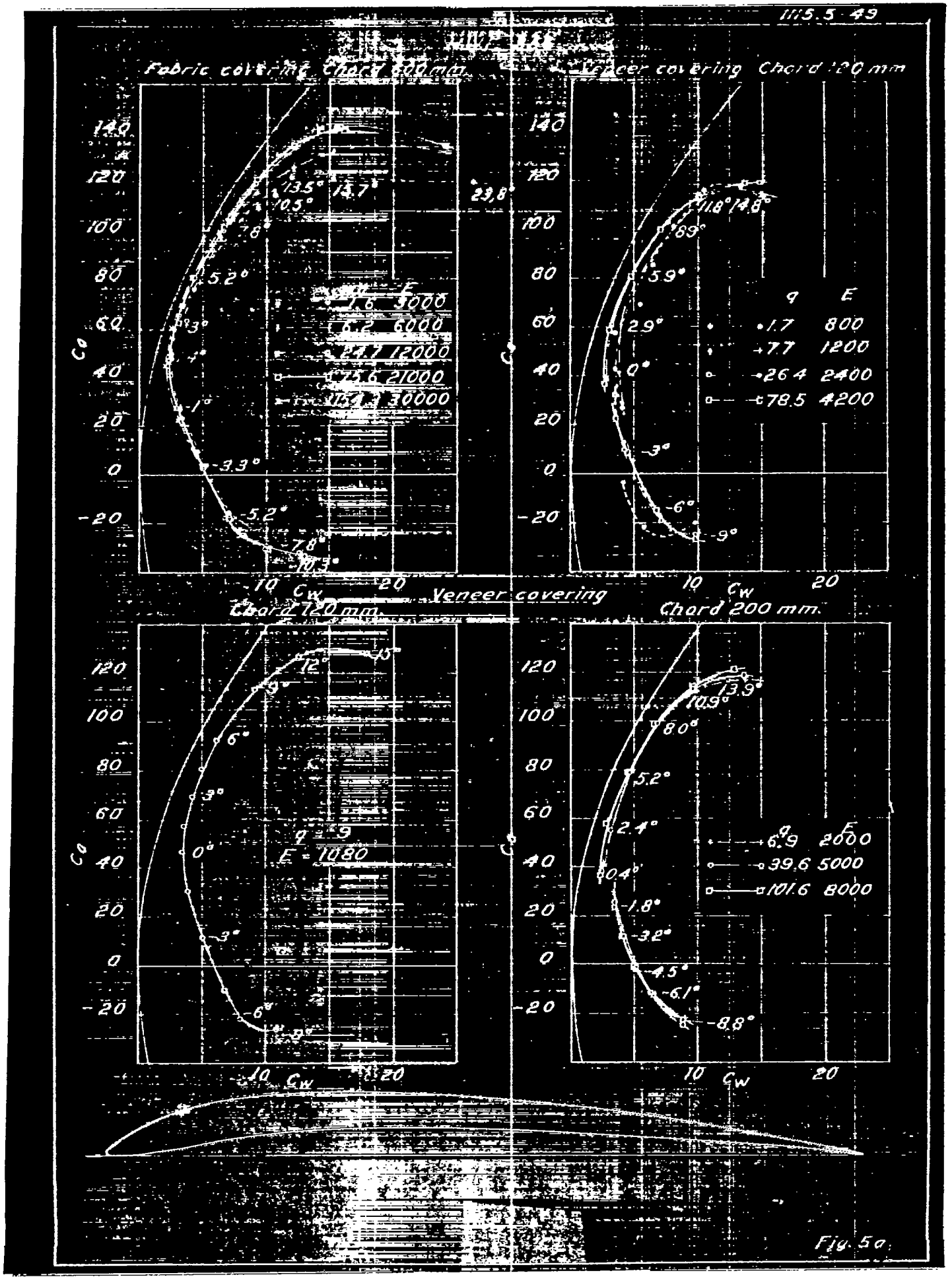
Fabric covering Chord 200 mm.
Veneer covering Chord 200 mm
Cl
Cw
q E
1.6 3000
6.2 6000
24.7 12000
25.6 21000
75.7 30000
1.7 800
7.7 1200
26.4 2400
78.5 4200
Veneer covering
Chord 120 mm.
Chord 200 mm.
q = 9
E = 1080
6.9 2000
39.6 5000
101.6 8000

Fig. 50.

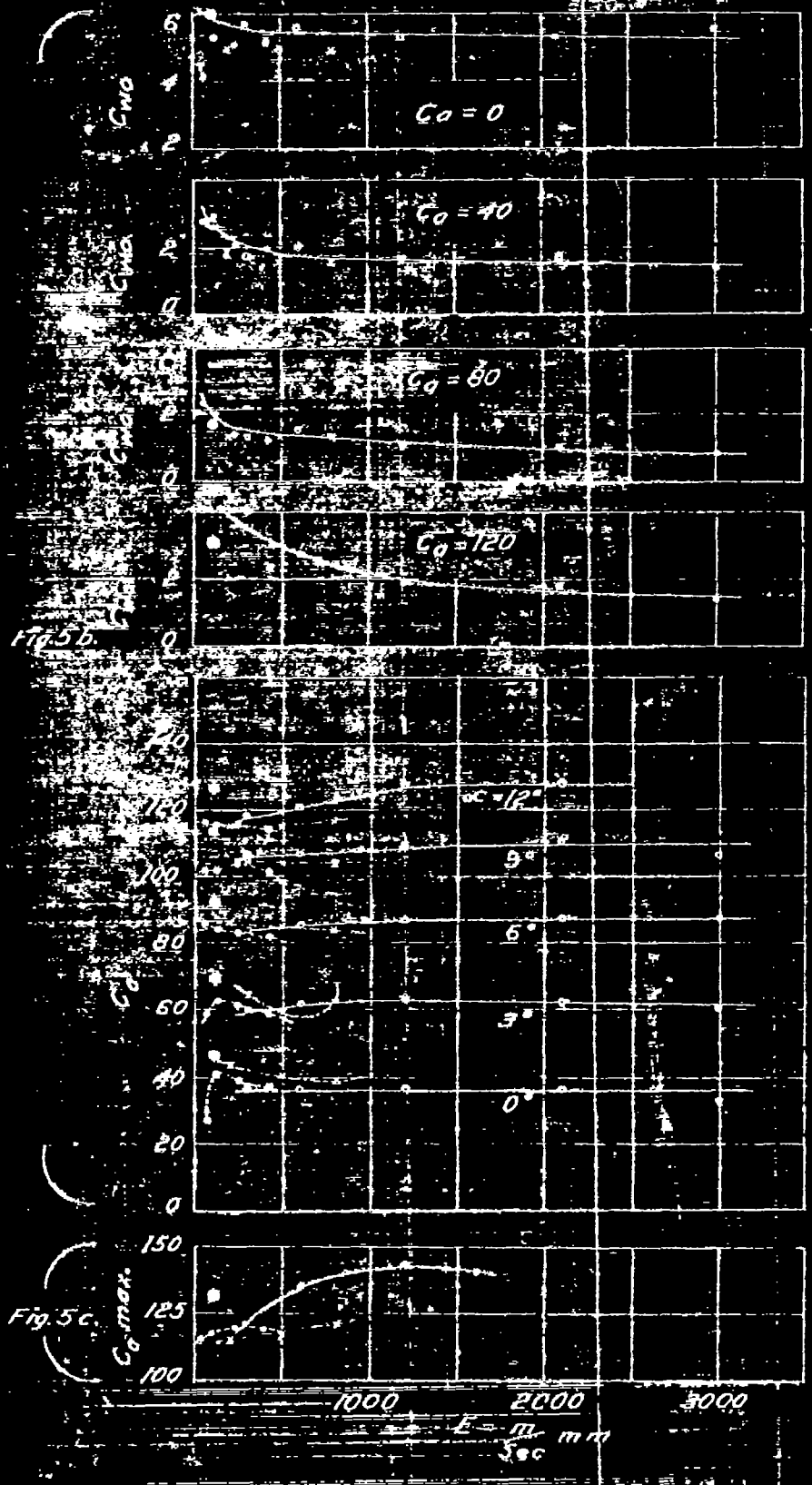

- t = 120 mm. Old Instillation
- t = 120 mm.
- x t = 200 mm. } New Instillation
- t = 600 mm.

Fig. 5b, 5c.

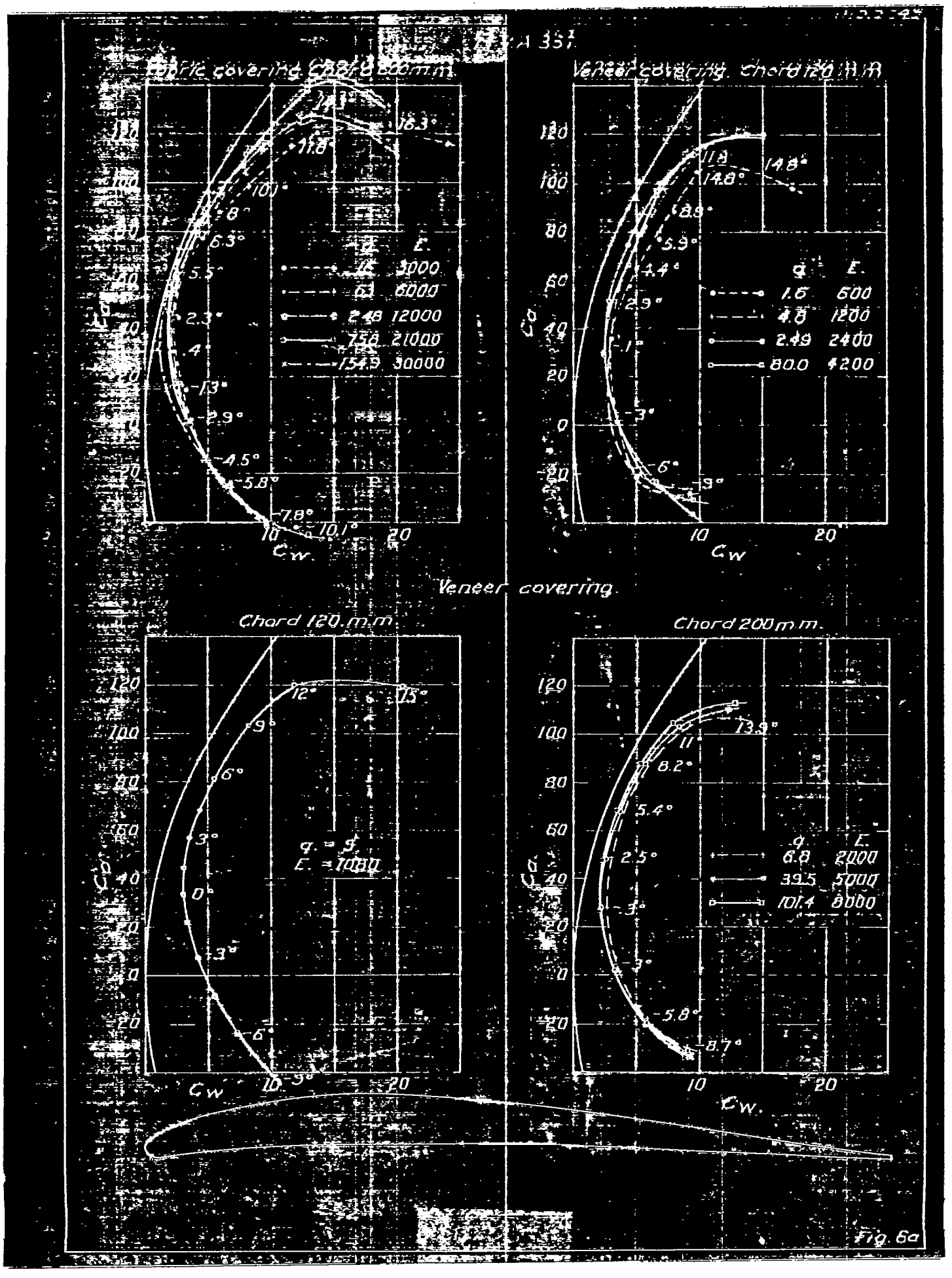
A 351
Fabric covering. Chord 200 m.m.
16.3°
11.8°
10°
8°
6.3°
5.5°
2.3°
-.4°
-1.3°
-2.9°
-4.5°
-5.8°
-7.8°
-10.1°
q E.
3.0 3000
6.1 6000
12.8 12000
75.8 21000
154.9 30000
Cw.
Veneer covering. Chord 120 m.m.
14.8°
14.8°
8.8°
5.9°
4.4°
2.9°
1.1°
-3°
-6°
-9°
q E.
1.6 600
4.8 1200
24.9 2400
80.0 4200
Cw
Veneer covering.
Chord 120 m.m.
12°
9°
6°
3°
0°
-3°
-6°
q = 9
E. = 1080
Cw
10.9°
Chord 200 m.m.
13.9°
11°
8.2°
5.4°
2.5°
-.3°
-3°
-5.8°
-8.7°
q E.
6.8 2000
39.5 5000
101.4 8000
Cw.
Fig. 6a

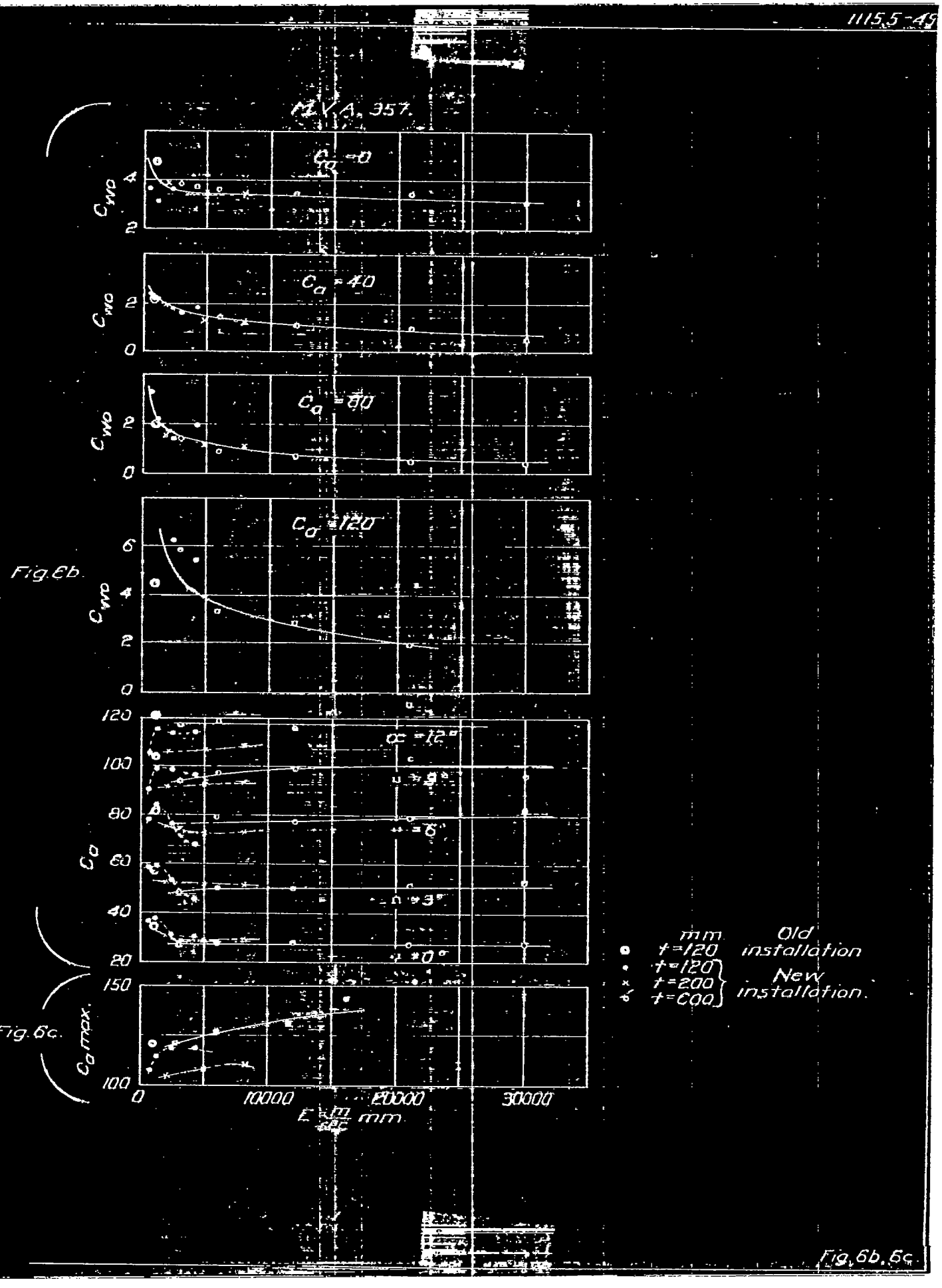

Fig. 6b.

Fig. 6c.

Fig. 6b. 6c.

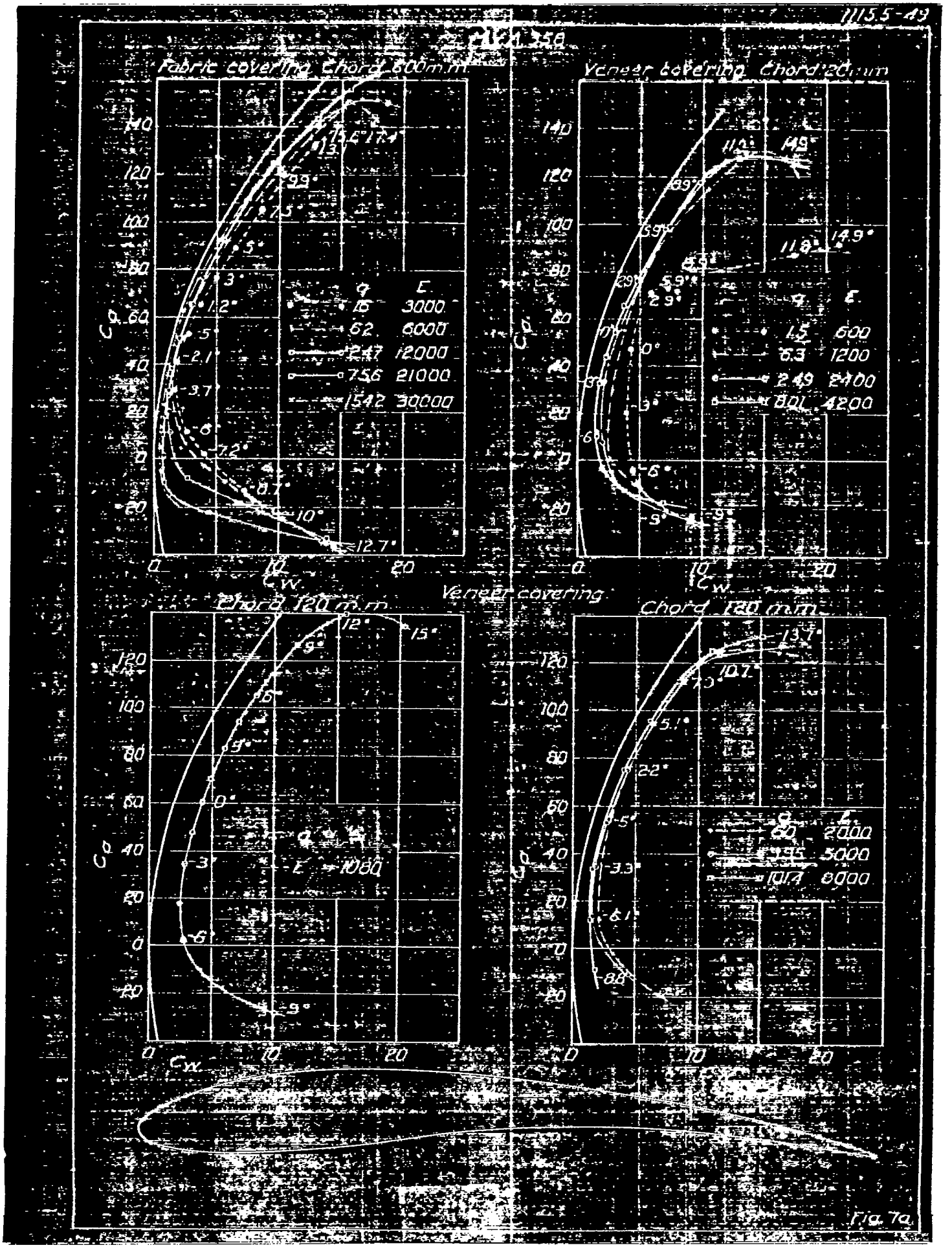
Fabric covering Chord 600 m.m.
Veneer covering Chord 240 m.m.
Veneer covering
Chord 120 m.m.
Chord 120 m.m.
q E
16 3000
62 6000
247 12000
756 21000
1542 30000
1.5 600
6.3 1200
24.9 2400
80.1 4200
E 1080
2.0 2000
9.95 5000
10.14 8000
Cw.
Cp.
Fig. 7a.

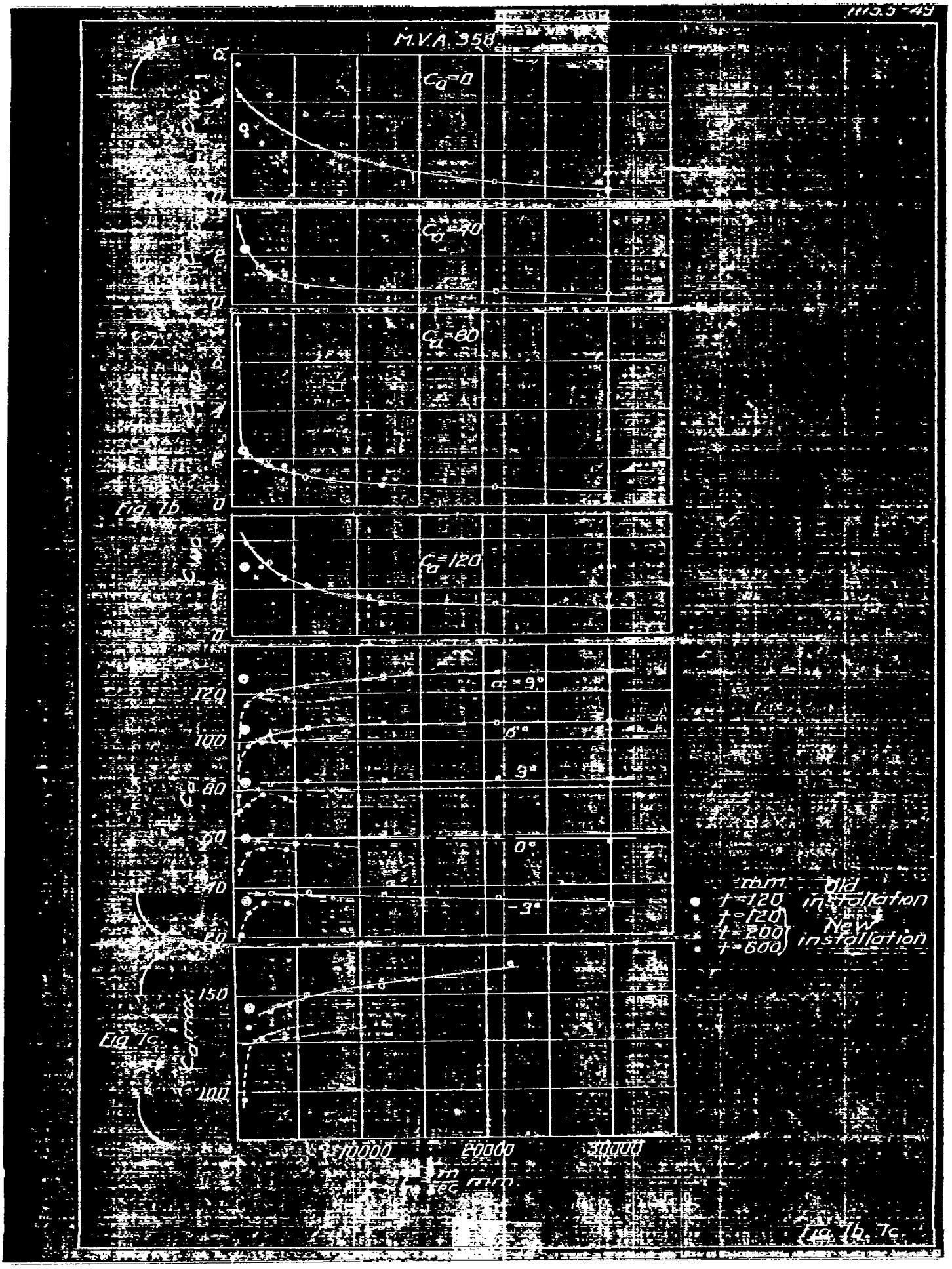
M.V.A. 358
α
C_a=0
C_a=40
C_a=80
C_a=120
$C_{a\,max}$
Fig. 7b
α = 9°
6°
3°
0°
-3°
mm old installation
t=120
t=120
t=200
t=600
new installation
150
100
Fig. 7c
10000
20000
30000
m
sec
m.p.h.
Fig. 7b, 7c.

K.W.W. 354

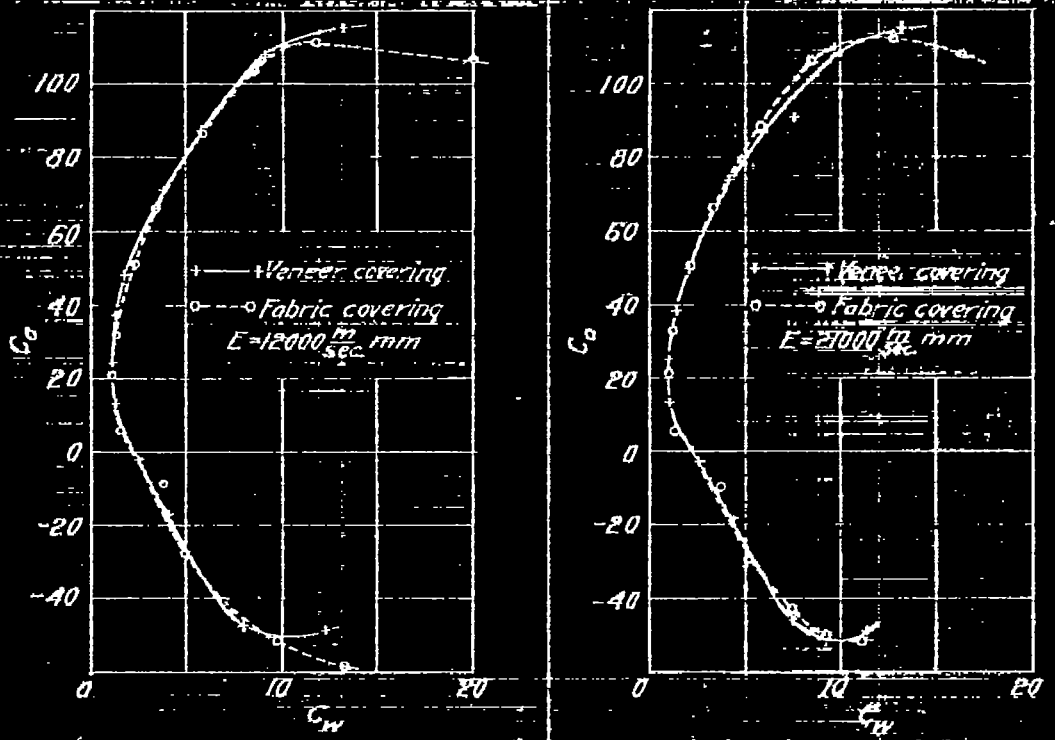

Fig. 8 Preceptable effect of sag in fabric due to air-force.

Fig. 8